

Accurate and Reliable Forecasting using Stochastic Differential Equations

Peng Cui¹ Zhijie Deng¹ Wenbo Hu² Jun Zhu¹

Abstract

It is critical yet challenging for deep learning models to properly characterize uncertainty that is pervasive in real-world environments. Although a lot of efforts have been made, such as heteroscedastic neural networks (HNNs), little work has demonstrated satisfactory practicability due to the different levels of compromise on learning efficiency, quality of uncertainty estimates, and predictive performance. Moreover, existing HNNs typically fail to construct an explicit interaction between the prediction and its associated uncertainty. This paper aims to remedy these issues by developing SDE-HNN, a new heteroscedastic neural network equipped with stochastic differential equations (SDE) to characterize the interaction between the predictive mean and variance of HNNs for accurate and reliable regression. Theoretically, we show the existence and uniqueness of the solution to the devised neural SDE. Moreover, based on the bias-variance trade-off for the optimization in SDE-HNN, we design an enhanced numerical SDE solver to improve the learning stability. Finally, to more systematically evaluate the predictive uncertainty, we present two new diagnostic uncertainty metrics. Experiments on the challenging datasets show that our method significantly outperforms the state-of-the-art baselines in terms of both predictive performance and uncertainty quantification, delivering well-calibrated and sharp prediction intervals.

1. Introduction

Deep neural networks (DNNs) are the *defacto* machine learning (ML) tools and significantly outperform human experts in terms of accuracy in various applications (LeCun et al., 2015; He et al., 2016; Vaswani et al., 2017; Devlin et al., 2018). However, considering the ubiquitous uncer-

¹Dept. of Comp. Sci., Tsinghua University, Beijing, China. ²RealAI, Beijing, China. Correspondence to: Peng Cui <xpeng.cui@gmail.com>, Jun Zhu <dcsjz@tsinghua.edu.cn>.

tainty in the real world, the high accuracy alone is routinely inadequate. As widely discussed, the accurate and reliable quantification of uncertainty is increasingly important for a variety of ML systems, e.g., autonomous driving (Michelmore et al., 2020), hydrological forecast (Klotz et al., 2020), medical diagnosis (Begoli et al., 2019) and business demand forecast (Zhu & Laptev, 2017). Typically, the uncertainty of particular concern is classified into two categories: *Aleatoric* uncertainty and *Epistemic* uncertainty a.k.a. data uncertainty and model uncertainty (Kendall & Gal, 2017). For regression tasks, the problem of uncertainty quantification mainly reduces to the estimation of prediction intervals (PIs), which is crucial for better-informed decisions (Pearce et al., 2018).

Heteroscedastic neural networks (HNNs) (Nix & Weigend, 1994) have long been an effective approach for uncertainty estimation in deep regression, which deliver the predictive mean and variance of the observation simultaneously. Despite simplicity and scalability, HNNs may exist a bias in fitting the data because of the possible misspecification of model parameters (Dybowski & Roberts, 2001), which lead to mis-calibrated prediction intervals. The pioneering works (Kendall & Gal, 2017; Lakshminarayanan et al., 2017) to enhance HNNs for more systematical uncertainty modeling typically draw inspiration from Bayesian neural networks (BNNs), while BNNs themselves are not problemless: 1) the high-dimensional parameters and the over-parameterization nature of DNNs pose fundamental challenges for effective posterior inference, thus unsatisfactory performance (Wenzel et al., 2020a) and degraded uncertainty estimates (Fort et al., 2019) are frequently observed; 2) empirical Bayesian methods like Deep Ensemble (Lakshminarayanan et al., 2017; Wenzel et al., 2020b), despite more flexible, are still restrictive in aspects of computation and memory complexity. Furthermore, unfortunately, rare of the variants of HNNs have succeeded in establishing a principled interaction between the predictive mean and variance, attributed to the conditional independence assumption between the two quantities. A direct consequence is that the prediction (i.e., predictive mean) and the associated uncertainty (i.e., predictive variance) cannot interact with each other directly, which contradicts the common sense of decision making.

This work aims to remedy the aforementioned issues of HNNs to realise more accurate and more reliable regression.

Our core insight is that there is an inherent alignment between the predictive mean & variance in HNNs and the drift & diffusion coefficients in a stochastic differential equation (SDE). Based on this insight, we present SDE-HNN, which incorporates the SDE into HNNs to construct an explicit and principled connection between the predictive mean and variance during the process of solving the SDE. Thereby, SDE-HNN enables a mutual boosting between the two aspects of predictive distribution during the optimization process, which is not enjoyed by the existing neural SDE methods for uncertainty quantification (Kong et al., 2020). In theory, we contribute an analysis on the existence and uniqueness of the solution to the devised neural SDE. Moreover, inspired by the bias-variance trade-off, we propose a variant of the Euler-Murayama (Klöden & Platen, 1992) method to discretize and solve the devised SDE, which works in light of dropout (Srivastava et al., 2014).

Intuitively, the model uncertainty characterized by the SDE is naturally integrated with the data uncertainty conveyed by the HNNs, yielding an efficient alternative for the combination of BNNs and HNNs. For the flexible adoption of the proposed method in practice, we further wrap the building and solving details of the neural SDE to constitute drop-in replacements for DNN blocks.

In practice, we usually expect the prediction intervals (PIs) given by the regressors not only to firmly cover the ground truth (calibration), but also as tight as possible (sharpness). To holistically evaluate the predictive uncertainty of different models, we propose two new diagnostic metrics: the confidence-weighted calibration error (CWCE) and its variant R-CWCE. Empirically, our method establishes a new state-of-the-art on challenging, large-scale time-series forecasting tasks, presenting remarkable improvement over competitive baselines in terms of both accuracy and uncertainty quantification, and producing high-quality PIs.

2. Related Work

As widely criticized, deep neural networks (DNNs) frequently suffer from over-fitting and are prone to yield over-confident predictions because they characterize the deterministic relationships between the observations and the targets of interest regardless of the other uncertain factors. As a compensation, Bayesian deep learning aims at equipping expressive DNNs with appropriate uncertainty quantification (Balan et al., 2015; Wang & Yeung, 2016; Kendall & Gal, 2017), with Bayesian neural networks (BNNs) as popular examples. Typically, BNNs perform the rigorous Bayesian inference over the high-dimensional network weights (Graves, 2011; Welling & Teh, 2011; Blundell et al., 2015; Liu & Wang, 2016; Sun et al., 2017; Louizos & Welling, 2017; Zhang et al., 2018; Khan et al., 2018; Osawa et al., 2019). Yet, it is widely observed that BNNs suffer

from the difficulty of prior specification (Sun et al., 2019), inevitably added training overhead when employing flexible variational posteriors (Shi et al., 2018), as well as the curse of dimensionality when resorting to sampling-based inference (Neal, 1995), which undermine the promise of Bayes principle. Empirical BNNs, e.g., Monte Carlo (MC) dropout (Gal & Ghahramani, 2016), Deep Ensemble (Lakshminarayanan et al., 2017), SWAG (Maddox et al., 2019), and BatchEnsemble (Wen et al., 2020) enjoy higher scalability and more outperforming predictive performance, but bear undesirable problems like degenerated uncertainty estimates (Fort et al., 2019), expensive training/storage cost, and limited expressiveness, etc. These issues together raise the requirement of a more efficient and more practically reliable uncertainty quantification paradigm to get the accurate and reliable regression.

Inspired by the motion of particles under environmental disturbances in stochastic differential equations (SDE), we suggest constructing the interaction between the prediction and the inherent uncertainty in HNNs to achieve more reliable regression. Existing work has made a step towards combining SDE with DNNs for uncertainty quantification (Kong et al., 2020). However, on the one hand, Kong et al. (2020) optimize the drift network and diffusion network in a separate, alternative manner, which may be deviated from the Euler-Murayama method for solving SDE and cannot construct the explicit connection between the predictive mean and variance for HNNs. On the other hand, they mainly focus on the out-of-distribution (OOD) detection task based on OOD training data and ignore to explicitly evaluate uncertainty in a principled way. The proposed approach differs from it in that we directly work on improving the uncertainty quantification and predictive accuracy for the deep regression by simulating the information flow under data and model perturbation in HNNs using SDEs, and develop an efficient numerical solver to deal with the devised neural SDE.

3. Preliminaries

In this section, we briefly review the background of heteroscedastic neural networks and stochastic differential equations.

3.1. Heteroscedastic Neural Networks

To arm DNNs with uncertainty estimation, a straightforward approach is to refine the DNNs to output the prediction value and the associated uncertainty concurrently. In this spirit, Nix & Weigend (1994) first introduce the heteroscedastic regression network based on heteroscedastic theory (Engle, 1982), which assumes a diagonal Gaussian predictive distribution and outputs the mean \hat{y} and variance σ^2 at the same

time:

$$[\hat{y}, \sigma^2] = I(x, \theta), \quad (1)$$

where I is a heteroscedastic neural network (HNN) parameterized by θ . Nevertheless, there is evidence to suggest that HNNs tend to suffer from the misspecification of model parameters, and hence miscalibrated predictive uncertainty (Dybowski & Roberts, 2001). Moreover, although HNNs can be substantially boosted by the advances in Bayesian deep learning (Kendall & Gal, 2017; Lakshminarayanan et al., 2017), most of the variants of HNNs ignore to explicitly characterize the influence of the associated uncertainty on the made prediction, leading to the fact that the predictive mean and variance merely have a weak interaction through the loss function. Motivated by Brownian motion which is used to model the randomness of particles in physics (Morters & Peres, 2010), we argue that it is necessary to explicitly construct a principled interaction between predictive mean and variance for uncertainty quantification in regression problems. To be specific, we establish the interaction by incorporating stochastic differential equations into HNNs base on the perspective of a stochastic dynamical system.

3.2. Stochastic Differential Equations

In order to simulate realistic dynamic systems with uncertainty, we can add some appropriate disturbance to deterministic differential equations, which is represented as:

$$\frac{dx_t}{dt} = f(x_t, t) + g(x_t, t) * \text{noise}. \quad (2)$$

When the noise term connects to Brown motion (Einstein et al., 1905) – the standard tool for uncertainty modeling, the above equation boils down to the Itô SDE (Itô, 1951):

$$dx_t = f(x_t) dt + g(x_t) dB_t. \quad (3)$$

Where B_t denotes a standard Brownian motion, and $f(\cdot)$ and $g(\cdot)$ refer to the drift coefficient and diffusion coefficient respectively. The principled interaction between the motion of particles (i.e., dx_t) and environmental disturbances (i.e., $dB(t)$) in the SDE inspires us to construct a connection between the predictive mean and variance in HNNs for regression problems.

4. SDE-HNN: An Improved Framework for Accurate and Reliable Regression

In this section, we first describe a framework to incorporate stochastic differential equations into the HNNs to achieve a practical and reliable uncertainty quantification in regression tasks. Then, we give a theoretical guarantee to show the existence and uniqueness of the solution to SDE-HNN (Theorem 1). Furthermore, from the perspective of bias-variance trade-off (Theorem 2), we present some theoretical under-

standings on the solving process of the neural SDE, and design a variant of the Euler-Maruyama method to improve the learning stability.

4.1. Reliable Regression via SDE-HNNs

Problem Setting. Considering a typical regression or forecasting task, we assume access to a dataset $\{(x^{(i)}, y^{(i)})\}_{i=1}^N$, with $x^{(i)} \in \mathbb{R}^d$ and $y^{(i)} \in \mathbb{R}$ denoting the d -dimension data and the target, respectively. The learning objective is to fit a Θ -parameterized regressor $H: x \rightarrow y$ according to the data. We denote by $p(y|x^{(i)})$ the predictive distribution corresponding to the regressor or forecaster for some data point $x^{(i)}$. The cumulative distribution function (CDF) F_i of such a distribution is informative for quantifying uncertainty – its inverse $F_i^{-1}: [0, 1] \rightarrow \hat{y}^{(i)}$ rigorously serves as the quantile function:

$$F_i^{-1}(p) = \inf \{y : p \leq F_i(y)\}. \quad (4)$$

In this work, in order to get accurate and reliable regression, we leverage the SDE to construct an explicit connection between predictive mean and variance in HNNs. Concretely, we deploy a neural SDE on the hidden representation z of the input x :

$$dz_t = f(z_t, \Theta_f) dt + g(z_t, \Theta_g) dB_t, \quad (5)$$

where t represents time. The functions $f(\cdot)$ and $g(\cdot)$ denote the drift and diffusion networks parameterized by Θ_f and Θ_g respectively, which are utilized to estimate the predictive mean and variance, so the interaction between the predictive mean and variance is constructed in the time-continuous dynamic system. Viewing this dynamic discretely, z_t refers to the state at the t -th implicit layer and the parameters are shared among layers.

HNNs output the different variance $\hat{\sigma}^2(x^{(i)})$ for each input $x^{(i)}$ base on the heteroscedastic theory (Engle, 1982). Correspondingly, in our setting, the predictive mean $\mu(x^{(i)})$ and variance $\sigma(x^{(i)})$ can be estimated as follows:

$$\begin{aligned} \mu(x^{(i)}) &= h_1(z_T^{(i)}, \Theta_{h_1}), \\ \sigma^2(x^{(i)}) &= h_2(g(z_T^{(i)}), \Theta_{h_2}), \end{aligned} \quad (6)$$

where h_1 and h_2 are two different linear layers (i.e., the mean layer and variance layer in Fig.1) parameterized by Θ_{h_1} and Θ_{h_2} respectively and $z_T^{(i)}$ is the equilibrium state of the hidden representation for input $x^{(i)}$. We drive the neural SDE to fit the data by minimizing negative log-likelihood loss (NLL):

$$L(\Theta_f; \Theta_g) = \sum_{i=1}^N \frac{\log \sigma^2(x^{(i)})}{2} + \frac{(y^{(i)} - \mu(x^{(i)}))^2}{2\sigma^2(x^{(i)})} + \text{constant}. \quad (7)$$

Empirically, to improve numerical stability, we can mini-

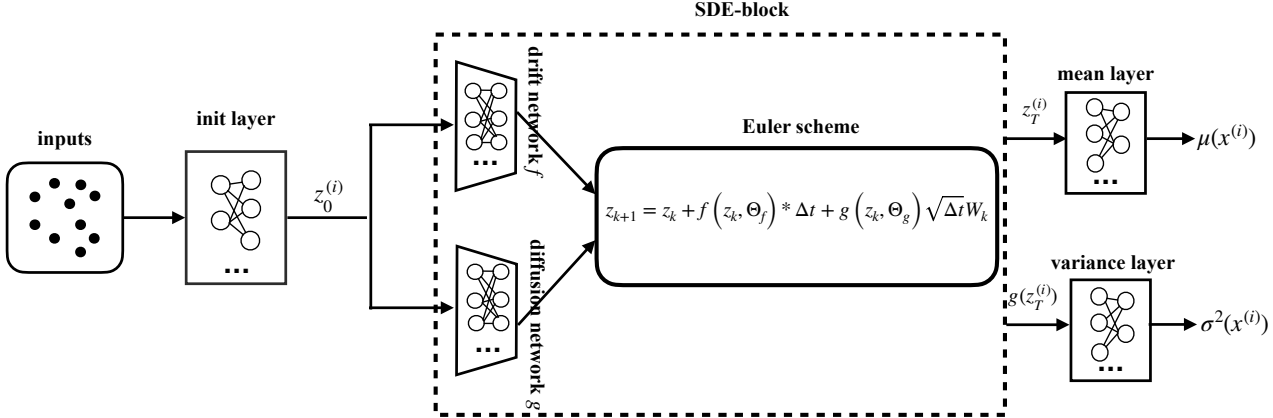


Figure 1. An illustration of SDE-HNN, which mainly includes three parts — the init layer, the SDE-block and the output layers (i.e., the mean layer and variance layer). The original HNNs do not have the intermediate SDE-block module. The SDE-block can simulate the explicit interaction between the predictive mean and variance during the solving process of SDE.

imize:

$$L(\Theta_f; \Theta_g) = \sum_{i=1}^N \frac{(y^{(i)} - \mu(x^{(i)}))^2}{2} \exp(-s^{(i)}) + \frac{1}{2}s^{(i)}, \quad (8)$$

where $s^{(i)} := \log \sigma^2(x^{(i)})$.

The Existence and Uniqueness of Solutions. In order to ensure that the constructed interaction is beneficial for both accuracy and uncertainty quantification in our framework, we need to make sure that the solution to the incorporated SDE exists. Analogous to the previous works on neural SDE (Kong et al., 2020), we theoretically show the existence and uniqueness of the solution to the neural SDE in our framework.

Theorem 1. (Proof in Appendix A) Suppose that $f(x_t, \Theta_f)$ and $g(x_t, \Theta_g)$ uniformly satisfy the Lipschitz condition, i.e., there exists a constant $K > 0$ making the following inequality hold:

$$\begin{aligned} & \|f(m, \Theta_f) - f(n, \Theta_f)\| + \|g(m, \Theta_g) - g(n, \Theta_g)\| \\ & \leq K\|m - n\|, \quad \forall m, n \in \mathbb{R}^d, t \geq 0. \end{aligned} \quad (9)$$

Then the stochastic differential equations have the unique solution.

Consequently, to make the neural SDE valid and solvable, we need to guarantee that the neural functions $f(x_t, \Theta_f)$ and $g(x_t, \Theta_g)$ uniformly satisfy the Lipschitz condition. To this end, we apply the well-evaluated spectral normalization trick (Miyato et al., 2018) to the weight matrix in the networks $f(\cdot)$ and $g(\cdot)$.

Solve the Neural SDE. In general, there is no close-form solution for SDE. We need to discretize the SDE and resort to numerical methods to iteratively approach the optimal solution. The process of solving SDE can actually be viewed as simulating the dynamic corresponding to this

SDE. A typical approach we can take is the Euler-Murayama method (Klöden & Platen, 1992), which iteratively applies the following transformation:

$$z_{k+1} = z_k + f(z_k, \Theta_f)(t_{k+1} - t_k) + g(z_k, \Theta_g)(B_{t+1} - B_t),$$

where k is the index of Euler iterations, with z_0 as some initial representation of the input x . According to the properties of the Brownian motion (Durrett, 2019): $B_{t+1} - B_t \sim \mathcal{N}(0, t_{k+1} - t_k)$, then we have $B_{k+1} - B_k = \sqrt{\Delta t} W_k$, where W_k follows the standard normal distribution. Therefore, we can rewrite the above transformation:

$$z_{k+1} = z_k + f(z_k, \Theta_f) \Delta t + g(z_k, \Theta_g) \sqrt{\Delta t} W_k, \quad (10)$$

where Δt is the step size of iterations. Let the terminal time of the stochastic process equal to T and the number of iterations equal to M , then $\Delta t = T/M$ and the final solution is z_T . Intuitively, T can be regarded as the number of implicit layers in SDE-HNN.

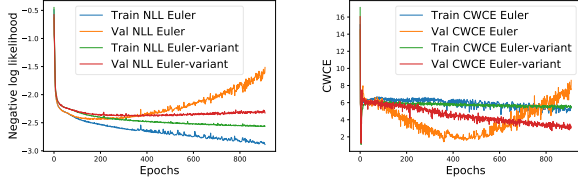
Our framework is shown in Fig.1, where the Euler solution process can be directly plugged into HNNs as an SDE-block without complicated model modification. The solving process follows the forward and backward propagation of DNNs and can be easily implemented with deep learning libraries. The $f(\cdot)$ and $g(\cdot)$ used to estimate the predictive mean and variance are jointly optimized in our framework. As a consequence, the prediction and the associated uncertainty can be interacted with each other in hidden features in a principle way. In contrast, the separate optimization for $f(\cdot)$ and $g(\cdot)$ in Kong et al. (2020) cannot construct such an interaction.

Uncertainty Quantification. Once the model has been trained, we can effectively capture both *Aleatoric* uncertainty and *Epistemic* uncertainty. To be specific, we can get a set of M sampled predictions: $\{\mu(x^{(i)}), \sigma^2(x^{(i)})\}_{m=1}^M$, and then compute the two kind of uncertainties with the

samples via

$$Ale(x^{(i)}) = \frac{1}{M} \sum_{m=1}^M \sigma_m^2(x^{(i)}).$$

$$Epi(x^{(i)}) = \frac{1}{M} \sum_{m=1}^M \mu_m(x^{(i)})^2 - \left(\frac{1}{M} \sum_{m=1}^M \mu_m(x^{(i)}) \right)^2.$$



(a) The NLL comparison of two solving methods. (b) The CWCE comparison of two solving methods.

Figure 2. Plotting the changing curve of NLL and CWCE on training data and validation data on the metro-traffic dataset. The CWCE is a metric of uncertainty evaluation defined in Sec.5.3

4.2. An Improved Solver Motivated By Bias-variance Tradeoff

We empirically find that the training process may become unstable when the network is close to convergence. This phenomenon can be interpreted by the bias-variance tradeoff that exists in the joint optimization process of $f(\cdot)$ and $g(\cdot)$. We give the following analysis and present an improved solver,

Theorem 2. *(Proof in Appendix B)* Given a dataset $\{(x_i, y_i)\}_{i=1}^K$ of size K , we assume that the training error of the model on this dataset is a constant. In our setting, the quantile function of the model that we want to learn from the dataset is $F^{-1}(p; x)$, dubbed as \mathcal{F} for brevity. There is a bias-variance tradeoff in the process of solving the neural SDE, that is, $MSE(\mathcal{F}, y) = Var_{(x, y)}(\mathcal{F}) + Bias_{(x, y)}(\mathbb{E}_{(x, y)}(\mathcal{F}), y)^2$

Because \mathcal{F} is derived from the distribution function (CDF), and the quantile p is stochastic, the output of \mathcal{F} corresponds to a stochastic output sampled from the SDE at each time t . The $Bias(E(\mathcal{F}), y)^2$ will gradually decrease as the network converges, and then $Var(\mathcal{F})$ will increase because of the constant assumption of $MSE(\mathcal{F}, y)$. The variance is mainly controlled by $g(\cdot)$ in our optimization procedure, so the training process will become unstable because of the increasing $g(\cdot)$. In order to improve the stability of network and make the network asymptotically converge to the optimal point for both mean and variance in the regression, we propose a variant of the standard Euler-Maruyama method. Specifically, we convert the original deterministic Gaussian uncertainty into Bernoulli's Gaussian uncertainty in the Euler-Maruyama equation to restrain possible explosive

$g(\cdot)$, which has the following form:

$$z_{k+1} = z_k + f(z_k, \Theta_f) \Delta t + \mathcal{D}(g(z_k, \Theta_g)) \sqrt{\Delta t} W_k.$$

Because the diffusion network $g(\cdot)$ has only one layer in our framework, we can simply utilize the Dropout (Srivastava et al., 2014) technique to realize the proposed approach in neural networks. Specifically, $\mathcal{D}(\cdot)$ can be regarded as applying dropout to the network $g(\cdot)$, so the Gaussian uncertainty is added with probability p during each Euler iteration, where p is the probability of the neuron being masked. Fig.2 shows the changing curve of NLL and CWCE (the CWCE is a metric of uncertainty evaluation defined in Sec.5.3) at training time, we can observe that the proposed variant of the Euler-Maruyama method is stabler than the standard Euler-Maruyama and can stably achieve better accuracy and uncertainty estimation performance on the validation dataset. In contrast, the original Euler method may cause the NLL to overfit to the training dataset, resulting in unstable training and poor predictive uncertainty performance.

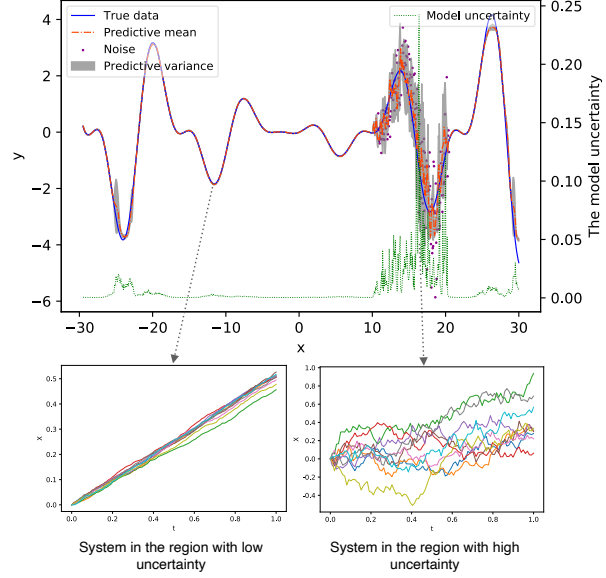


Figure 3. Results on a synthetic dataset, the proposed method can quantify two types of uncertainties simultaneously (the predictive variance corresponds to the data uncertainty). The trajectories of the system are scattered in the region with noise (the right figure at the bottom), oppositely, trajectories of the system are stable in the region with deterministic function (the left figure at the bottom).

5. Experimental Results

In this section, we first evaluate the behavior of the proposed method qualitatively on synthetic data. Secondly, we compare the proposed method with heteroscedastic neural networks and other strong baselines on challenging and large-scale time series forecasting tasks in terms of prediction accuracy and predictive uncertainty. It is commonly recognized that time series forecasting is a crucial and complicated task in data science and machine learning,

which needs to model multiple regression sub-problems in sequence. Last but not least, we show that the computation efficiency of the proposed method compared with the baseline methods.

5.1. Toy example

We firstly qualitatively and visually show the behavior of the proposed method on a one-dimensional synthetic dataset. The synthetic dataset consists of 1000 data points, where the independent variable x is uniformly sampled within $[-30, 40]$ and the dependent variable y is obtained via the function $y = (0.4x) \times \sin x + (0.7x) \times \cos x/2$. Moreover, we add the heteroscedastic Gaussian noise ϵ_t within $[10, 20]$ via the function to observe the behavior of the dynamic system and network, where $\epsilon \sim \mathcal{N}(0, 0.0225x^2)$. Knowing the true noise in our synthetic dataset, we can evaluate the quality of predictive uncertainty.

We use the model with 64 units in all hidden layers (the init layer, drift network $f(\cdot)$ and diffusion network $g(\cdot)$). The terminal time T and step size Δt of Euler solver are set to 3 and 1 respectively. The results are shown in Fig.3. We can observe that the predictive variance (data uncertainty) becomes higher in the area where heteroscedastic Gaussian noise is added within $[10, 20]$ and the model uncertainty can increase within $[10, 20]$ because the made prediction is not too exact in the area. The two figures in Fig.3 at the bottom show that ten trajectories sampled from another linear SDE. If the system is in the region with clean data and deterministic pattern, the system is stable. On the contrary, if the system is in the region with noise, the diffusion coefficient is high, the system becomes disordered.

5.2. Setup

Datasets. We conduct our experiments on public multivariate time series data from UCI repository (Dua), Kaggle (Yan) and Lai et al. (2018). A multivariate time series data consists of multiple time-dependent variables, it is more challenging due to the complex mixtures of temporal patterns and inter-dependencies among multivariate time series. Table 2 describes the details of the datasets in Appendix D.

Baselines. We compare the proposed method with several competitive and popular baselines, including heteroscedastic neural network (HNN) (Kendall & Gal, 2017), MC-Dropout (MCD) (Gal & Ghahramani, 2016), Deep Ensembles (Deep-ens) (Lakshminarayanan et al., 2017), Deep Gaussian Processes (DGP) (Salimbeni & Deisenroth, 2017) and BNN (Blundell et al., 2015).

Model setting and hyperparameters. In our experiments, we split each of the six datasets into training data (60%), validation data (20%) and testing data (20%). For the model architecture, we construct an LSTM model with

two hidden layers (both 128 hidden units) and two linear layers to make the final predictions for all baselines. Fairly, the init layer of the proposed method is one-layer LSTM with 64 hidden units, the drift network f and the diffusion network g are both one-layer LSTM with 64 hidden units. The terminal time T and step size Δt of the Euler solver are set to 3 and 0.5 respectively.

For the data preprocessing, we scale the raw data into the range $[0,1]$ to improve the computation stability and efficiency. And we choose the size of the sliding window is 5 and the forecasting horizon is 1 according to validation datasets. Take the Metro-traffic dataset as an example, the traffic volume data of the past five hours is used to predict the data of one hour in the future. For optimization algorithm, we all use the Adam (Kingma & Ba, 2014) with learning rate 10^{-3} and weight decay 10^{-3} . For all experimental results, we report the averaged results obtained from 5 random trials.

5.3. Evaluation metrics.

Formally, we say a regressor is *well-calibrated* (Dawid, 1982; Kuleshov et al., 2018) if for $\forall p \in [0, 1]$, the following condition always holds:

$$\frac{\sum_{i=1}^N \mathbb{I}\{y_i \leq F_i^{-1}(p)\}}{N} \rightarrow p, \text{ when } N \rightarrow \infty, \quad (11)$$

where $\mathbb{I}(\cdot)$ is the indicator function that equals to 1 if the predicate holds otherwise 0. The left terms in Eqn. (11) is generally referred to as the empirical coverage probability, dubbed as $E(p)$.

In the previous literature, for real-world applications of machine learning, the predictive uncertainty is evaluated from two aspects: calibration and sharpness (Gneiting et al., 2007).

Proposed confidence-weighted calibration metric. The calibration metrics are traditionally defined through the quantile function for regression problems. In the previous works (Dawid, 1982; Kuleshov et al., 2018; Cui et al., 2020), the calibration error is the equivalent accumulation of different quantile (confidence) deviation, which may be inaccurate when the data distribution is uneven. For the realistic usage, the quantile deviation with a large confidence is more important than those with a small confidence. To overcome this issue, we propose a new metric, confidence-weighted calibration error (CWCE), which is defined as:

$$\text{CWCE} = \sum_{k=1}^n p_k \times |E(p_k) - p_k|, \quad (12)$$

where $E(q)$ is the empirical coverage probability and p is the true confidence (i.e., the confidence level that we expect).

Dataset	Metric	MCD	DGP	BNN	Deep-ens	HNN	Proposed
Metro-traffic	RMSE	697.021	651.341	786.694	533.426	559.354	483.639±2.657
	$R^2 \uparrow$	0.877	0.892	0.843	0.928	0.920	0.939±0.011
	CWCE	52.152	10.552	21.486	9.078	9.305	2.894±0.085
	EPIW	<i>167.859</i>	1168.044	610.662	814.143	883.475	539.254±19.334
	R-CWCE	6.428	1.136	3.373	0.655	0.747	0.177±0.014
Pickups	RMSE	625.812	523.041	720.013	428.032	421.752	340.331±5.072
	$R^2 \uparrow$	0.878	0.914	0.838	0.943	0.945	0.964±0.012
	CWCE	34.441	22.799	42.570	4.878	6.043	2.925±0.758
	EPIW	<i>313.432</i>	1872.481	247.229	684.381	688.989	438.324±19.222
	R-CWCE	4.205	1.951	6.904	0.280	0.335	0.173±0.012
Stock	RMSE	4.947	3.530	8.663	2.122	1.903	2.102±0.024
	$R^2 \uparrow$	0.993	0.997	0.981	0.999	0.998	0.999±0.000
	CWCE	5.869	26.911	15.233	14.678	18.430	3.717±0.069
	EPIW	6.421	15.839	29.882	4.273	4.208	3.303±0.058
	R-CWCE	0.039	0.084	0.285	0.017	0.020	0.004±0.000
Electricity	RMSE	3780.973	2936.760	6106.273	1535.261	1592.815	1497.891±10.253
	$R^2 \uparrow$	0.642	0.739	0.415	0.887	0.884	0.894±0.003
	CWCE	49.138	9.225	47.096	5.575	4.169	3.555±0.297
	EPIW	<i>156.028</i>	492.443	<i>345.186</i>	382.168	379.107	358.012±4.778
	R-CWCE	17.585	2.405	27.571	0.630	0.486	0.378±0.005
Solar	RMSE	3.405	2.995	3.813	1.982	2.201	1.940±0.006
	$R^2 \uparrow$	0.890	0.938	0.855	0.965	0.964	0.966±0.001
	CWCE	62.528	9.103	9.1840	18.568	12.081	8.403±1.684
	EPIW	<i>0.296</i>	2.996	2.650	1.749	1.946	2.418±0.222
	R-CWCE	6.890	0.569	1.334	0.657	0.439	0.288±0.002
Traffic flow	RMSE	0.040	0.047	0.047	0.023	0.024	0.022±0.000
	$R^2 \uparrow$	0.393	0.213	0.112	0.786	0.782	0.813±0.000
	CWCE	55.490	27.229	46.959	14.554	12.706	10.464±0.931
	EPIW	<i>0.004</i>	0.030	<i>0.011</i>	0.024	0.024	0.021±0.001
	R-CWCE	33.700	21.419	41.688	3.109	2.766	1.956±0.001

Table 1. The forecast accuracy, calibration error and sharpness of uncertainty evaluation for each method on different datasets. Each column represents the performance of a specific method for different metrics on different datasets. The larger values represent better performance in the metric with ' \uparrow '. Note that when the corresponding CWCE and RMSE are too large, EPIW has no comparative meaning with other methods and these EPIWs are written in *italics*.

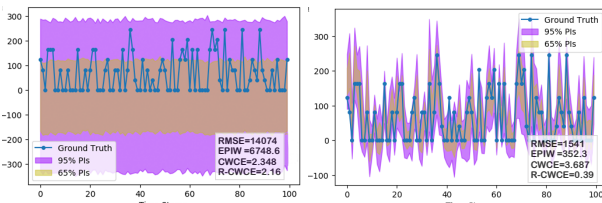


Figure 4. The partial prediction intervals comparison at the 65% and 95% confidence on the electricity dataset. The CWCE and EPIW are equal to 2.348 and 6748.6 in the left figure, and the CWCE and EPIW are equal to 3.687 and 352.3 in the right figure. The definitions of EPIW can be found in Appendix E.

Proposed metric for fusing calibration and sharpness. Generally, we prefer prediction intervals are as tight as possible when accurately covering the ground truths (i.e., the calibration error is low). At the moment, the sharpness should be considered as a diagnostic tool for uncertainty, which refers to the concentration of the predictive distributions (Gneiting et al., 2007). The calibration and sharpness are evaluated separately in the previous works (Kuleshov

et al., 2018; Pearce et al., 2018; Cui et al., 2020), so we need to consider both metrics respectively when comparing the results. For convenience, in this paper, we design a combinative metric to evaluate the calibration and sharpness together. Motivated by the coefficient of determination, we propose R-CWCE, the variant of CWCE:

$$R\text{-CWCE} = \frac{\sum_i (y_i - \hat{y}_i)^2}{\sum_i (y_i - \bar{y})^2} \times CWCE, \quad (13)$$

where \hat{y}_i is the predictive mean of the model, \bar{y} is the mean of the observed data, the first term of the right of the equation represents the predictive performance of the model. A smaller R-CWCE represents better calibration and sharpness performance, the value of R-CWCE on the left (2.16) is obviously greater than that (0.39) on the right in Fig.4, which shows that the proposed metric is more effective.

In summary, the performance of all methods is evaluated from two aspects, the precision of prediction and the reliabil-

bility of uncertainty: 1) the metrics of prediction precision: RMSE and R^2 , 2) the metrics of the calibration and sharpness: CWCE, R-CWCE and EPIW, where the definitions of RMSE, R^2 and EPIW can be found in Appendix E.

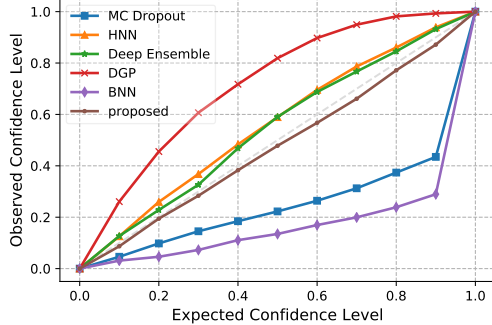


Figure 5. Plots of the empirical coverage probability vs expected confidence for all methods on Pickups dataset.

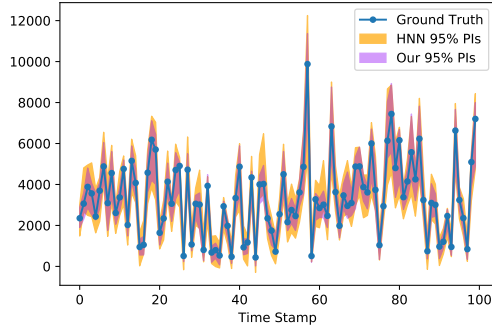


Figure 6. The comparison plots of prediction intervals between HNN and our method on Pickups dataset.

5.4. Time Series Forecasting on real world datasets

Table 1 shows the performance of prediction precision and uncertainty reliability for all methods. We can observe that the proposed method significantly outperforms the baselines in terms of the metrics of forecasting and uncertainty estimation by achieving lower RMSE and calibration error (CWCE). And the R-CWCE of the proposed method is the smallest on all datasets, which shows the effectiveness of the proposed method for both the calibration and sharpness. Especially, the proposed method achieves a great performance improvement in both forecasting and uncertainty estimation compared to HNNs and also greatly outperforms competitive Deep-Ensembles. In order to visually demonstrate the performance of uncertainty estimation, we report calibration curves and prediction intervals in Fig.5 and Fig.6. Fig.5 shows the empirical coverage probability at different confidence levels, the result of the proposed model is closest to the expected confidence level, which indicates the best calibration performance among all methods. Fig.6 shows 95% prediction intervals obtained by the proposed method and HNNs, the intervals are visually sharper and can accurately

cover the ground truths, which show the proposed method can output well-calibrated and sharp prediction intervals.

5.5. Computation Efficiency

We analyze the computational efficiency of all methods on the stock dataset, including the number of parameters and training time. The experimental settings are consistent with Sec. 5.4. As can be seen in Fig.7, Deep Ensemble has the maximum number of parameters and is the most time-consuming. Bayesian methods (i.e., DGP and BNNs) also have a high computational cost. By contrast, the training time and parameters of the proposed method are the least among all methods.

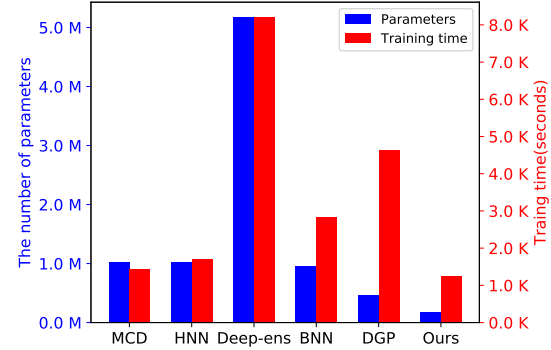


Figure 7. The number of parameters and training time of all methods on stock dataset on GTX1080Ti.

6. Conclusions and Future Work

In this work, we present SDE-HNN, a practical and efficient method that incorporates stochastic differential equations (SDE) to explicitly characterize the interaction between the predictive mean and variance of HNNs. We show the existence and uniqueness of the solution for our method, provide an analysis for the optimization process based on bias-variance trade-off, and further design a variant of the Euler-Maruyama method to improve the learning stability. Finally, we reexamine the current uncertainty evaluation and propose two new diagnostic metrics. Empirically, our method significantly outperforms the competitive baselines in terms of both predictive accuracy and uncertainty quantification on the non-trivial real datasets.

Because the plug-and-play *SDE-block* is sufficiently flexible in our framework, in future work, we will be devoted to promoting the proposed method and framework to more tasks to get well-calibrated predictions, such as classification and detection. Another worthwhile investigation is the combination of our method and other calibration methods, such as temperature scaling (Guo et al., 2017), non-parametric isotonic regression (Kuleshov et al., 2018) and distribution matching (Cui et al., 2020), to further improve the uncertainty quantification in classification and regression tasks.

References

UCI machine learning repository. <http://archive.ics.uci.edu/ml>. Accessed: 2020-06-04.

Nyc uber pickups with weather and holidays — kaggle. <https://www.kaggle.com/yannisp/uber-pickups-enriched>. Accessed: 2020-06-04.

Balan, A. K., Rathod, V., Murphy, K. P., and Welling, M. Bayesian dark knowledge. In *Advances in Neural Information Processing Systems*, pp. 3438–3446, 2015.

Begoli, E., Bhattacharya, T., and Kusnezov, D. The need for uncertainty quantification in machine-assisted medical decision making. *Nature Machine Intelligence*, 1(1):20–23, 2019.

Blundell, C., Cornebise, J., Kavukcuoglu, K., and Wierstra, D. Weight uncertainty in neural networks. In *Proceedings of the 32nd International Conference on International Conference on Machine Learning-Volume 37*, pp. 1613–1622, 2015.

Cui, P., Hu, W., and Zhu, J. Calibrated reliable regression using maximum mean discrepancy. *Advances in Neural Information Processing Systems*, 33, 2020.

Dawid, A. P. The well-calibrated Bayesian. *Journal of the American Statistical Association*, 77(379):605–610, 1982.

Devlin, J., Chang, M.-W., Lee, K., and Toutanova, K. Bert: Pre-training of deep bidirectional transformers for language understanding. *arXiv preprint arXiv:1810.04805*, 2018.

Durrett, R. *Probability: theory and examples*, volume 49. Cambridge university press, 2019.

Dybowski, R. and Roberts, S. J. Confidence intervals and prediction intervals for feed-forward neural networks. *Clinical applications of artificial neural networks*, pp. 298–326, 2001.

Einstein, A. et al. On the motion of small particles suspended in liquids at rest required by the molecular-kinetic theory of heat. *Annalen der physik*, 17(549-560):208, 1905.

Engle, R. F. Autoregressive conditional heteroscedasticity with estimates of the variance of united kingdom inflation. *Econometrica: Journal of the Econometric Society*, pp. 987–1007, 1982.

Fort, S., Hu, H., and Lakshminarayanan, B. Deep ensembles: A loss landscape perspective. *arXiv preprint arXiv:1912.02757*, 2019.

Gal, Y. and Ghahramani, Z. Dropout as a Bayesian approximation: Representing model uncertainty in deep learning. In *international conference on machine learning*, pp. 1050–1059, 2016.

Gneiting, T., Balabdaoui, F., and Raftery, A. E. Probabilistic forecasts, calibration and sharpness. *Journal of the Royal Statistical Society: Series B (Statistical Methodology)*, 69(2):243–268, 2007.

Graves, A. Practical variational inference for neural networks. In *Advances in Neural Information Processing Systems*, pp. 2348–2356, 2011.

Guo, C., Pleiss, G., Sun, Y., and Weinberger, K. Q. On calibration of modern neural networks. In *International Conference on Machine Learning*, pp. 1321–1330, 2017.

He, K., Zhang, X., Ren, S., and Sun, J. Deep residual learning for image recognition. In *Proceedings of the IEEE conference on computer vision and pattern recognition*, pp. 770–778, 2016.

Itô, K. *On stochastic differential equations*. Number 4. American Mathematical Soc., 1951.

Kendall, A. and Gal, Y. What uncertainties do we need in Bayesian deep learning for computer vision? *Advances in neural information processing systems*, pp. 5574–5584, 2017.

Khan, M. E., Nielsen, D., Tangkaratt, V., Lin, W., Gal, Y., and Srivastava, A. Fast and scalable Bayesian deep learning by weight-perturbation in adam. In *International Conference on Machine Learning*, pp. 2616–2625, 2018.

Kingma, D. P. and Ba, J. Adam: A method for stochastic optimization. *arXiv preprint arXiv:1412.6980*, 2014.

Klöden, P. E. and Platen, E. Numerical solution of stochastic differential equations. 1992.

Klotz, D., Kratzert, F., Gauch, M., Sampson, A. K., Klam-bauer, G., Hochreiter, S., and Nearing, G. Uncertainty estimation with deep learning for rainfall-runoff modelling. *arXiv preprint arXiv:2012.14295*, 2020.

Kong, L., Sun, J., and Zhang, C. Sde-net: Equipping deep neural networks with uncertainty estimates. In *International Conference on Machine Learning*, pp. 5405–5415. PMLR, 2020.

Kuleshov, V., Fenner, N., and Ermon, S. Accurate uncertainties for deep learning using calibrated regression. *International Conference on Machine Learning*, pp. 2796–2804, 2018.

Lai, G., Chang, W.-C., Yang, Y., and Liu, H. Modeling long- and short-term temporal patterns with deep neural networks. In *The 41st International ACM SIGIR Conference on Research & Development in Information Retrieval*, pp. 95–104, 2018.

Lakshminarayanan, B., Pritzel, A., and Blundell, C. Simple and scalable predictive uncertainty estimation using deep ensembles. *Advances in neural information processing systems*, pp. 6402–6413, 2017.

LeCun, Y., Bengio, Y., and Hinton, G. Deep learning. *nature*, 521(7553):436–444, 2015.

Liu, Q. and Wang, D. Stein variational gradient descent: A general purpose Bayesian inference algorithm. In *Advances in Neural Information Processing Systems*, pp. 2378–2386, 2016.

Louizos, C. and Welling, M. Multiplicative normalizing flows for variational Bayesian neural networks. In *International Conference on Machine Learning*, pp. 2218–2227, 2017.

Maddox, W. J., Izmailov, P., Garipov, T., Vetrov, D. P., and Wilson, A. G. A simple baseline for bayesian uncertainty in deep learning. In *Advances in Neural Information Processing Systems*, pp. 13153–13164, 2019.

Michelmore, R., Wicker, M., Laurenti, L., Cardelli, L., Gal, Y., and Kwiatkowska, M. Uncertainty quantification with statistical guarantees in end-to-end autonomous driving control. In *International Conference on Robotics and Automation*, 2020.

Miyato, T., Kataoka, T., Koyama, M., and Yoshida, Y. Spectral normalization for generative adversarial networks. In *International Conference on Learning Representations*, 2018.

Morters, P. and Peres, Y. Cambridge series in statistical and probabilistic mathematics, 2010.

Neal, R. M. *Bayesian Learning for Neural Networks*. PhD thesis, University of Toronto, 1995.

Nix, D. A. and Weigend, A. S. Estimating the mean and variance of the target probability distribution. In *Proceedings of 1994 ieee international conference on neural networks (ICNN'94)*, volume 1, pp. 55–60. IEEE, 1994.

Osawa, K., Swaroop, S., Jain, A., Eschenhagen, R., Turner, R. E., Yokota, R., and Khan, M. E. Practical deep learning with Bayesian principles. *arXiv preprint arXiv:1906.02506*, 2019.

Pearce, T., Brintrup, A., Zaki, M., and Neely, A. High-quality prediction intervals for deep learning: A distribution-free, ensembled approach. In *International Conference on Machine Learning*, pp. 4075–4084. PMLR, 2018.

Salimbeni, H. and Deisenroth, M. Doubly stochastic variational inference for deep gaussian processes. In *Advances in Neural Information Processing Systems*, pp. 4588–4599, 2017.

Shi, J., Sun, S., and Zhu, J. A spectral approach to gradient estimation for implicit distributions. *arXiv preprint arXiv:1806.02925*, 2018.

Srivastava, N., Hinton, G., Krizhevsky, A., Sutskever, I., and Salakhutdinov, R. Dropout: a simple way to prevent neural networks from overfitting. *The journal of machine learning research*, 15(1):1929–1958, 2014.

Sun, S., Chen, C., and Carin, L. Learning structured weight uncertainty in Bayesian neural networks. In *International Conference on Artificial Intelligence and Statistics*, pp. 1283–1292, 2017.

Sun, S., Zhang, G., Shi, J., and Grosse, R. Functional variational Bayesian neural networks. In *International Conference on Learning Representations*, 2019.

Vaswani, A., Shazeer, N., Parmar, N., Uszkoreit, J., Jones, L., Gomez, A. N., Kaiser, Ł., and Polosukhin, I. Attention is all you need. *Advances in neural information processing systems*, 30:5998–6008, 2017.

Wang, H. and Yeung, D.-Y. Towards Bayesian deep learning: A framework and some existing methods. *IEEE Transactions on Knowledge and Data Engineering*, 28(12):3395–3408, 2016.

Welling, M. and Teh, Y. W. Bayesian learning via stochastic gradient langevin dynamics. In *Proceedings of the 28th international conference on machine learning (ICML-11)*, pp. 681–688, 2011.

Wen, Y., Tran, D., and Ba, J. Batchensemble: an alternative approach to efficient ensemble and lifelong learning. *arXiv preprint arXiv:2002.06715*, 2020.

Wenzel, F., Roth, K., Veeling, B. S., Świątkowski, J., Tran, L., Mandt, S., Snoek, J., Salimans, T., Jenatton, R., and Nowozin, S. How good is the bayes posterior in deep neural networks really? *arXiv preprint arXiv:2002.02405*, 2020a.

Wenzel, F., Snoek, J., Tran, D., and Jenatton, R. Hyperparameter ensembles for robustness and uncertainty quantification. *Advances in Neural Information Processing Systems*, 33, 2020b.

Zhang, G., Sun, S., Duvenaud, D., and Grosse, R. Noisy natural gradient as variational inference. In *International Conference on Machine Learning*, pp. 5847–5856, 2018.

Zhu, L. and Laptev, N. Deep and confident prediction for time series at Uber. In *2017 IEEE International Conference on Data Mining Workshops (ICDMW)*, pp. 103–110. IEEE, 2017.

A. The proof of Theorem 1

Theorem 1 can be seen as a special case of the existence and uniqueness theorem of a general stochastic differential equation, we first introduce some lemmas.

Lemma 1. Let C_1, C_2, \dots be a sequence of events in the probability space. The Borel–Cantelli lemma states:

If the sum of the probabilities of the event E_n is finite,

$$\sum_{n=1}^{\infty} \Pr(C_n) < \infty, \quad (14)$$

then the probability that infinitely many of them occur is 0, that is,

$$\Pr\left(\limsup_{n \rightarrow \infty} C_n\right) = 0. \quad (15)$$

In the theorem 1, we declare that the stochastic differential equations have the unique solution,

$$dz_t = f(z_t; t; \Theta_f) dt + g(z_t; t; \Theta_g) dB_t, z_0 = z. \quad (16)$$

Firstly, we prove the uniqueness of solutions. Suppose y is another solution, that is,

$$dy_t = f(y_t; t; \Theta_f) dt + g(y_t; t; \Theta_g) dB_t, y_0 = z. \quad (17)$$

Then we calculate the square of the subtraction of Eqn.17 and Eqn.16, then use the basic inequality $(a + b)^2 \leq 2a^2 + 2b^2$ and take the expectation, we can get,

$$\begin{aligned} \mathbb{E}|y_t - z_t|^2 &\leq 2\mathbb{E}\left(\int_0^t (f(y_s) - f(z_s)) dB_s\right)^2 \\ &\quad + 2\mathbb{E}\left(\int_0^t (g(y_s) - g(z_s)) ds\right)^2 \\ &\leq 2\mathbb{E}\int_0^t |f(y_s) - f(z_s)|^2 d\langle B, B \rangle_s \\ &\quad + 2\mathbb{E}\left(t \int_0^t |g(y_s) - g(z_s)|^2 ds\right). \end{aligned} \quad (18)$$

According to the Lipschitz condition, we can get,

$$\mathbb{E}|y_t - z_t|^2 \leq 2K^2\mathbb{E}\int_0^t |y_s - z_s|^2 ds + 2K^2t\mathbb{E}\int_0^t |y_s - z_s|^2 ds. \quad (19)$$

Let $c(t) = \mathbb{E}|y_t - z_t|^2$, then for any $t \leq T$, we can get

$$c(t) \leq C_T \int_0^t c(s) ds, \quad (20)$$

where $C_T = 2K^2(1 + T)$, from the above inequality, we can immediately conclude that $c(t) = 0$, so the uniqueness holds.

Moreover, we use iterative methods to prove the existence and then define the following equation:

$$z_t^n = z + \int_0^t f(z_s^{n-1}) ds + \int_0^t g(z_s^{n-1}) ds. \quad (21)$$

We will prove the convergence of z^n . We take the subtraction of z_t^{n+1} and z_t^n , and then we can get,

$$\begin{aligned} \max_{0 \leq s \leq t} |z_s^{n+1} - z_s^n| &\leq 2 \max_{0 \leq s \leq t} \left(\int_0^s [f(z_u^n) - f(z_u^{n-1})] du \right)^2 \\ &\quad + 2TK^2 \int_0^t \max_{0 \leq u \leq s} |z_u^n - z_u^{n-1}| ds. \end{aligned} \quad (22)$$

Let $\eta_n(t) = \mathbb{E}[\max_{0 \leq s \leq t} |z_s^n - z_s^{n-1}|^2]$, from the moment inequality of Doob martingale, for any $t \leq T$,

$$\eta_{n+1}(t) \leq D_T \int_0^t \eta_n(s) ds. \quad (23)$$

Where $D_T = 2K^2(4 + T)$, let $C = \eta_1(T)$, we can get the following inequality by recursion,

$$\eta_n(T) \leq \frac{C(TD_T)^{n-1}}{(n-1)!}. \quad (24)$$

Based on Markov inequality: $P(x \geq a) \leq \frac{E(x)}{a}$ for $x \geq 0, a > 0$, we can get,

$$\sum_{n=1}^{\infty} \mathbb{P}\left[\max_{0 \leq s \leq T} |z_s^n - z_s^{n-1}| \geq 2^{-n}\right] < \infty. \quad (25)$$

According to Borel–Cantelli lemma 1, we can deduce that the limit $\lim_{n \rightarrow \infty} x_n$ exists, and the limit process is continuous. Because the above sequence also converges in the sense of L^2 , we can take the limit in the recursive equation to get,

$$dz_t = f(z_t; t; \Theta_f) dt + g(z_t; t; \Theta_g) dB_t. \quad (26)$$

Hence, the existence of the solution is proved.

B. The proof of Theorem 2

Proof. The generalization error of the quantile function \mathcal{F} with respect to the ground-truth can be computed as:

$$\begin{aligned} \text{MSE}(\mathcal{F}, y) &= \mathbb{E}_{(x,y)}[(\mathcal{F} - y_i)^2] \\ &= \mathbb{E}_{(x,y)}[(\mathcal{F} - \mathbb{E}_{(x,y)}(\mathcal{F}) + \mathbb{E}_{(x,y)}(\mathcal{F}) - y)^2] \\ &= \mathbb{E}_{(x,y)}[(\mathcal{F} - \mathbb{E}_{(x,y)}(\mathcal{F}))^2 + 2(\mathcal{F} - \mathbb{E}_{(x,y)}(\mathcal{F}))(\mathbb{E}_{(x,y)}(\mathcal{F}) - y) \\ &\quad + (\mathbb{E}_{(x,y)}(\mathcal{F}) - y)^2] \\ &= \mathbb{E}_{(x,y)}(\mathcal{F} - \mathbb{E}_{(x,y)}(\mathcal{F}))^2 + \mathbb{E}_{(x,y)}[2(\mathcal{F} - \mathbb{E}_{(x,y)}(\mathcal{F})) \\ &\quad (\mathbb{E}_{(x,y)}(\mathcal{F}) - y)] + \mathbb{E}_{(x,y)}(\mathbb{E}(\mathcal{F}) - y)^2 \\ &= \mathbb{E}_{(x,y)}(\mathcal{F} - \mathbb{E}_{(x,y)}(\mathcal{F}))^2 + 2(\mathbb{E}_{(x,y)}(\mathcal{F}) - y) \\ &\quad \mathbb{E}_{(x,y)}(\mathcal{F} - \mathbb{E}_{(x,y)}(\mathcal{F})) + \mathbb{E}_{(x,y)}(\mathbb{E}_{(x,y)}(\mathcal{F}) - y)^2 \\ \text{MSE}(\mathcal{F}, y) &= \text{Var}_{(x,y)}(\mathcal{F}) + \text{Bias}_{(x,y)}(\mathbb{E}_{(x,y)}(\mathcal{F}), y)^2 \end{aligned}$$

C. Two Side Well Calibration

More practically, we usually a two-sided calibration to evaluate uncertainty. For a prediction interval (PI) $[F_i^{-1}(p_1), F_i^{-1}(p_2)]$, $\forall p_1 \in [0, 1], p_2 \in [p_1, 1]$, there is a similar definition for two-sided calibration:

$$\frac{\sum_{i=1}^N \mathbb{I}\{F_i^{-1}(p_1) \leq y_i \leq F_i^{-1}(p_2)\}}{N} \rightarrow p_2 - p_1, \quad (27)$$

holds as $N \rightarrow \infty$.

D. Datasets

Datasets	L	D	T
Metro-traffic	48204	9	1 hour
Pickups	29102	11	1 hour
Stock	40560	81	1 minute
Electricity	26304	321	1 hour
Solar	52560	137	10 minutes
Traffic flow	17544	862	1 hour

Table 2. The description of dataset used, where L is length of time-series or data size, D is number of variables, T is time interval among series.

E. Metrics

Prediction precision metrics. Root Mean Square Error (RMSE) is the standard deviation of the residuals (prediction errors), which is defined as follow:

$$\text{RMSE} = \sqrt{\frac{1}{n} \sum_{i=1}^n (y_i - \hat{y}_i)^2} \quad (28)$$

R^2 is also a common metric to evaluate forecasting performance, which is a real number in $[0, 1]$, the predictions are more accurate when R^2 is close to 1, which is defined as follow:

$$R^2 = 1 - \frac{\sum_i (y_i - \hat{y}_i)^2}{\sum_i (y_i - \bar{y})^2}, \quad (29)$$

Calibration metrics. In the previous works, the expectation of coverage probability error (ECPE) (Cui et al., 2020) of prediction intervals (PIs) is the absolute difference between true confidence and empirical coverage probability, which is defined as:

$$\text{ECPE} = \frac{1}{n} \sum_{j=1}^n |P_j - \hat{P}_j|. \quad (30)$$

Where P_j is the expected confidence (i.e., the confidence level that we expect), and \hat{P}_j is probability that prediction intervals cover the ground truth.

Sharpness metrics. A kind of sharpness is represented as the averaged width of the prediction intervals (EPIW) (Cui et al., 2020), which is defined as follow:

$$\text{EPIW} = \frac{1}{n} \sum_{j=1}^n \hat{Y}_{j\text{up}} - \hat{Y}_{j\text{low}}, \quad (31)$$

where n is the total number of prediction intervals, $\hat{Y}_{j\text{up}}, \hat{Y}_{j\text{low}}$ are the upper and lower bounds of prediction intervals respectively.